

# The worldwide NORM production and a fully automated gamma-ray spectrometer for their characterization

Khixha G.<sup>1,d,e,f</sup>, Bezzon G. P.<sup>b</sup>, Brogгинi C.<sup>a</sup>, Buso G. P.<sup>b</sup>, Caciolli A.<sup>a,c</sup>, Callegari I.<sup>c</sup>, De Bianchi S.<sup>d</sup>, Fiorentini G.<sup>b,d,e</sup>, Guastaldi E.<sup>c</sup>, Kaçeli Xhixha M.<sup>g</sup>, Mantovani F.<sup>d,e</sup>, Massa G.<sup>c</sup>, Menegazzo R.<sup>a</sup>, Mou L.<sup>c</sup>, Pasquini A.<sup>c</sup>, Rossi Alvarez C.<sup>a</sup>, Shyti M.<sup>d,e</sup>

<sup>a</sup> Istituto Nazionale di Fisica Nucleare (INFN), Padova Section, Via Marzolo 8 - 35131 Padova, Italy.

<sup>b</sup> Istituto Nazionale di Fisica Nucleare (INFN), Legnaro National Laboratory, Via dell'Università, 2 - 35020 Legnaro, Padova, Italy.

<sup>c</sup> University of Siena, Center for GeoTechnologies, Via Vetri Vecchi, 34 - 52027 San Giovanni Valdarno, Arezzo, Italy.

<sup>d</sup> University of Ferrara, Physics Department, Via Saragat, 1 - 44100 Ferrara, Italy.

<sup>e</sup> Istituto Nazionale di Fisica Nucleare (INFN), Ferrara Section, Via Saragat, 1 - 44100 Ferrara, Italy.

<sup>f</sup> Agricultural University of Tirana, Faculty of Forestry Science, Kodër Kamëz - 1029 Tirana, Albania.

<sup>g</sup> University of Sassari, Botanical, Ecological and Geological Sciences Department, Piazza Università 21- 07100 Sassari, Italy.

## Abstract

Materials containing radionuclides of natural origin and being subject to regulation because of their radioactivity are known as NORM (Naturally Occurring Radioactive Material). By following IAEA, we include in NORM those materials with an activity concentration, which is modified by human made processes. We present a brief review of the main categories of non-nuclear industries together with the levels of activity concentration in feed raw materials, products and waste, including mechanisms of radioisotope enrichments. The global management of NORM shows a high level of complexity, mainly due to different degrees of radioactivity enhancement and the huge amount of worldwide waste production. The future tendency of guidelines concerning environmental protection will require both a systematic monitoring based on the ever-increasing sampling and high performance of gamma ray spectroscopy. On the ground of these requirements a new low background fully automated high-resolution gamma-ray spectrometer MCA\_Rad has been developed. The design of lead and copper shielding allowed to reach a background reduction of two order of magnitude with respect to laboratory radioactivity. A severe lowering of manpower cost is obtained through a fully automation system, which enables up to 24 samples to be measured without any human attendance. Two coupled HPGe detectors increase the detection efficiency, performing accurate measurements on small sample volume (180 cc) with a reduction of sample transport cost of material. Details of the instrument calibration method are presented. MCA\_Rad system can measure in less than one hour a typical NORM sample enriched in U and Th with some hundreds of Bq/kg, with an overall uncertainty less than 5%. Quality control of this method has been tested. Measurements of three certified reference materials RGK-1, RGU-2 and RGTh-1 containing concentrations of potassium, uranium and thorium comparable to NORM have been performed. As a result, this test achieved an overall relative discrepancy of 5% among central values within the reported uncertainty.

**Keywords:** HPGe, Gamma-ray spectrometry, Industrial waste/by-product, NORM, Non-nuclear industry, Reference materials

## 1. Introduction

Materials containing radionuclides of natural origin and being subject to regulation because of their radioactivity are known as NORM (Naturally Occurring Radioactive Material).

---

<sup>1</sup>Khixha Gerti, Dipartimento di Fisica, Università di Ferrara, Polo Scientifico e Tecnologico Via Saragat, 1 – 44100 Ferrara, Italy. Phone: +39-3200864636, Fax: +39-0532974210, E-mail: khixha@fe.infn.it

By following IAEA, we include in NORM those materials with an activity concentration altered by human made processes<sup>2</sup> (IAEA, 2008; IAEA, 2003a). In the last decades the large production of NORM and the potential long-term radiological hazards, due to long-lived radionuclides, represented an increasing level of concern. The development of instruments devoted to the measurements of NORM concentrations is a crucial task for the evaluation of the radiological impact on both workers and public members.

NORM are found as products, by-products and/or wastes of industrial activities, such as production of non-nuclear fuels (e.g. coal, oil and gas), mining and milling of metalliferous and nonmetalliferous ores (e.g. aluminum, iron, copper, gold and mineral sand), industrial minerals (e.g. phosphate and clays), radioisotope extraction and processing, as well as water treatments (IAEA, 2003b).

The most important sources of natural radioactivity are due to the presence of  $^{238}\text{U}$ ,  $^{232}\text{Th}$  and  $^{40}\text{K}$  in the Earth. Generally  $^{235}\text{U}$  and  $^{87}\text{Rb}$  and other trace elements are negligible. The decay chain of  $^{238}\text{U}$  ( $^{232}\text{Th}$ ) includes 8 (6) alpha decays and 6 (4) beta decays respectively, which are often associated with gamma transitions. The detection of these radioactivity sources can be performed through a wide set of methods, such as gamma-ray spectroscopy, alpha spectroscopy, neutron activation analysis (NAA), inductively-couple plasma mass-spectroscopy (ICP-MS), inductively coupled plasma atomic emission spectroscopy (ICP-AES), X-ray fluorescence spectroscopy (XRF) and liquid scintillation counting (LSC) (IAEA, 2006). The choice of the methodology for determining radioactive content of NORM depends on many factors, especially the economic character and prompt measurement of the individual samples.

Usually, in NORM  $^{238}\text{U}$  and  $^{232}\text{Th}$  decay chains are not in secular equilibrium. It means that in  $^{238}\text{U}$  decay chain, some long lived radionuclides ( $^{238}\text{U}$ ,  $^{226}\text{Ra}$ ,  $^{210}\text{Pb}$ ) represent the head of decay chain segments, which can reach the secular equilibrium in less than one year: the gamma ray spectrometry, therefore, is the suitable technique for measuring the abundance of these radionuclides and for checking the secular equilibrium among the respective chain segments. NORM can be enriched in  $^{230}\text{Th}$  and  $^{210}\text{Po}$ , which can be out of chain segments: the activities of  $^{230}\text{Th}$  can be determined by gamma-spectrometry directly, while the suitable technique for quantifying  $^{210}\text{Po}$  concentration is alpha spectrometry. In  $^{232}\text{Th}$  decay chain the two chain segments, having on head  $^{228}\text{Ra}$  and  $^{228}\text{Th}$ , reach the secular equilibrium in about one month. By measuring the gamma transitions in each chain segment, one can determine  $^{228}\text{Ra}$  and  $^{228}\text{Th}$  abundances; while XRF, NAA, ICP-AES, ICP-MS are suitable techniques for measuring  $^{232}\text{Th}$  content.

By using high-resolution gamma-ray spectrometry, all radioisotopes of  $^{238}\text{U}$  and  $^{232}\text{Th}$  decay chains, with the exception of  $^{232}\text{Th}$  and  $^{210}\text{Po}$ , can be investigated simultaneously. The radioactivity characterization of NORM may require a massive amount of measures of samples. For this purpose we designed and built up a low background high-resolution gamma-ray spectrometry system, which allows an autonomous investigation of the radioactivity content on a large amount of samples, without any human attendance.

An empirical method for the characterization of the absolute efficiency of this instrument is presented in detail. Along with the instrument calibration, a quality test of this method was carried out. We tested the performances of the instrument by using three reference materials RGK-1, RGU-1 and RGTh-1 certified by International Atomic Energy Agency (IAEA) and containing radioactive concentration comparable to NORM values.

## 2. Industrial processes producing NORM: an overview

---

<sup>2</sup> Sometimes these materials are known in the literature as TENORM (technologically enhanced naturally occurring radioactive material).

## 2.1 Non-nuclear fuels extraction and processing

### *Oil and gas industry*

Most hydrocarbons are trapped within porous reservoirs (known as oil/tar sand and oil shale deposits) by impermeable rocks above: the rock formations holding the oil also contain U and Th at the order of some ppm, corresponding to a total specific activity of some tens<sup>3</sup> of Bq kg<sup>-1</sup>. Oil and gas reservoirs contain a natural water layer (formation water) that lies under the hydrocarbons: U and Th do not go into solution, but the formation water tends to reach a specific activity of the same order of the rock matrix ([Metz et al., 2003](#)) due to dissolution of <sup>226</sup>Ra and <sup>228</sup>Ra radium as radium chloride ([Heaton and Lambley, 1995](#)). Additional heated water is often injected into the reservoirs to achieve maximum oil recovery. This process disturbs the cation/anion ratio and alters the solubility of various sulfate salts, particularly BaSO<sub>4</sub> and RaSO<sub>4</sub>: radium co-precipitates with barium as sulfates forming scale within the oil pipes ([Jerez Vegueria et al., 2002](#)). The solids, which are dissolved in crude oil and in the produced water, precipitate forming the sludge, which is a mixture of oil, carbonates and silicates sediments, as well as corrosion products that accumulate inside piping and in the bottom of storage tanks. The contribution to the radioactivity content in the sludge comes mainly from the precipitates of hard insoluble radium sulphate and possibly from radioactive silts and clays ([Heaton and Lambley, 1995](#)). The specific activity of scales and sludges can vary enormously and generally it is of several orders of magnitude more than formation water. As reported in [Table 1](#), the high variability, often among the samples collected in the same area, shows that a frequent and dense sampling of these NORM may be required.

### *Coal-fired power plant*

Coal is a combustible sedimentary rock formed through the anaerobic process of the decomposed dead plants accumulated at the bottom of basins of some marsh land, lake or sea: the coalification process yields a product rich in carbon and hydrogen ([Rubio Montero et al., 2009](#)). The organic matter plays an important role in the uranium concentrations at syngenetic, epigenetic and diagenetic stages of the sedimentary cycle ([Nakashima, 1992](#)). The complexation and reduction of uranium are considered the main geochemical processes of the fixation of uranium on organic matter from very dilute solutions. The complexation of uranium involves the uranyl cation (UO<sub>2</sub><sup>2+</sup>) producing a UO<sub>2</sub> complex through a dehydrogenation process of organic matter. During the reduction of the soluble UO<sub>2</sub><sup>2+</sup>, the insoluble UO<sub>2</sub> is produced precipitating as uraninite ([Landais, 1996](#)). The efficiency of these processes depends on the chemistry of the organic matter and on the temperature of reaction, producing U concentrations ranged over a couple orders of magnitude: the typical range of radionuclide activity concentrations of <sup>238</sup>U, <sup>232</sup>Th and <sup>40</sup>K in coal can be 10-600 Bq kg<sup>-1</sup>, 10-200 Bq kg<sup>-1</sup> and 30-100 Bq kg<sup>-1</sup> respectively ([Beck, 1989](#)). The geological processes over the time increase the grade of coal transforming the organic material from peat to graphite. In low-grade coal the secular equilibrium between <sup>238</sup>U and <sup>232</sup>Th and their decay products is not expected while in the high-grade coal it may exist ([Tadmor, 1986](#)). The volatilization–condensation process of particles during coal combustion breaks the secular equilibrium and increases the radionuclide concentrations with decreasing of particle size: the maximum enrichment has been measured in particles with diameters of about 1 μm. <sup>210</sup>Pb and <sup>210</sup>Po exhibit the greatest enrichment, as much as a factor of 5, while maximum

---

<sup>3</sup> The U and Th abundances vary for different rock types: e.g. in considering shale, the range of U and Th abundances reported by ([Condie, 1993](#)) are 2.4-3.4 ppm and 8.5-14.3 ppm respectively. We remind that the specific activity of 1 ppm U (Th) corresponds to 12.35 (4.06) Bq/kg.

enrichment for uranium isotopes is about a factor of 2, and for  $^{226}\text{Ra}$  a factor of around 1.5. In some samples of fly ash the  $^{210}\text{Pb}$  and  $^{226}\text{Ra}$  activity exceeds thousands of  $\text{Bq kg}^{-1}$  (Flues, 2006).

According to the World Coal Institute (WCI, 2005) 40% of the world's electricity in 2003 is generated by coal: in the same year the world coal consumption reached  $48.4 \cdot 10^{11}$  kg (U.S. EIA / IEO, 2010). After the combustion of the bituminous coal containing an average ash of 12%, coal by-products are composed by some 70% of fly ash and by some 30% of the bottom ash and boiler slag. A large fraction (more than 95%) of these small particles can be removed from gas stream, by usually applying electrostatic precipitator and fabric filters: in 2003 the estimated worldwide fly ash production was  $3.9 \cdot 10^{11}$  kg (Mukherjee et al., 2008). In 2003 the US and EU fly ash production was about  $0.6 \cdot 10^{11}$  kg and  $0.4 \cdot 10^{11}$  kg respectively. In US and UE about 39% and 48% of this amount was recycled respectively (ACAA, 2003; ECOBA, 2003). According to (U.S. EIA / IEO, 2010) the world coal consumption in 2035 is projected to reach  $93.8 \cdot 10^{11}$  kg, corresponding to an estimated fly ash production of  $7.5 \cdot 10^{11}$  kg. This large amount of NORM is required to be measured and monitored with accuracy, by developing fast and *ad hoc* methods: the MCA\_Rad system presented in section 3 has been designed as a response to this increasing demand.

**Table 1.** Range of specific activity concentrations of  $^{226}\text{Ra}$  and  $^{228}\text{Ra}$  in scale and sludge, as reported by different authors for various geographic regions. Remind that the exemption level recommended by (IAEA, 1996) is  $10^4$   $\text{Bq kg}^{-1}$  for both  $^{226}\text{Ra}$  and  $^{228}\text{Ra}$ .

Authors of the study	Country	$^{226}\text{Ra}$ [ $10^4$ $\text{Bq kg}^{-1}$ ]		$^{228}\text{Ra}$ [ $10^4$ $\text{Bq kg}^{-1}$ ]	
		Scale	Sludge	Scale	Sludge
Godoy and Cruz, 2003	Brazil	1.91 – 32.3	0.036 – 36.7	0.421 – 23.5	0.025 – 34.3
Gazineu et al., 2005a	Brazil	12.1 – 95.5	0.24 – 350	13.1 – 79.2	205
Gazineu and Hazin, 2008	Brazil	7.79 – 211	0.81 – 41.3	10.2 – 155	0.94 – 11.8
Shawky et al., 2001	Egypt	0.754 – 14.3	0.0018	3.55 – 66.1	1.33
Abo-Elmagd et al., 2010	Egypt	49.3 – 51.9	0.527 – 0.886	3.20 – 5	0.1 – 0.19
Bakr, 2010	Egypt	0.0016 – 0.0315	0.00055 – 0.179	0.00007 – 0.0177	0.00007 – 0.0885
Omar et al., 2004	Malaysia	0.055 – 43.4	0.0006 – 0.056	0.09 – 47.9	0.0004 – 0.052
Lysebo et al., 1996	Norway	0.03 – 3.23	0.03 – 3.35	0.01 – 0.47	0.01 – 0.46
Al-Saleh and Al-Harshan, 2008	Saudi Arabia	0.00008 – 0.00015	0.00068 – 0.00594	0.000014 – 0.00031	0.00063 – 0.00476
Al-Masri and Suman, 2003	Syria	14.7 – 105	47 – 100	4.3 – 18.1	35.9 – 66
Jonkers et al., 1997	USA	0.01 – 1500	0.005 – 80	0.005 – 280	0.05 – 50
Zielinski et al., 2001	USA	1.88 – 489	2.04 – 6.38	0.118 – 19	0.241 – 0.574

## 2.2 Metal mineral extraction and processing

### Bauxite extraction and alumina production

In metal mining and waste processing, the radioactive content varies from  $10^{-2}$  kBq kg<sup>-1</sup>, for the large volume industry, to  $10^2$  kBq kg<sup>-1</sup> for rare earth metals (IAEA, 2003b). In massive metal extraction, the amount of NORM produced by bauxite processing is relevant.

Bauxites generally contain concentrations of Th and U greater than the Earth's crustal average: in a multi-methodological study published by (Adams and Richardson, 1960) based on twenty-nine samples of bauxites from different locations, the reported specific activities of U and Th are in the range 33 – 330 Bq kg<sup>-1</sup> and 20 – 532 Bq kg<sup>-1</sup> respectively. These values can be compared with the typical concentration in bauxite: 400 – 600 Bq kg<sup>-1</sup> for U and 300 – 400 Bq kg<sup>-1</sup> for Th (UNSCEAR, 2000).

The parent rocks affect the U and Th abundances in the bauxites: in particular the bauxites derived from acid igneous rocks show a concentration higher than those extracted from basic igneous rocks, whereas the bauxites mined from deposits of shales and carbonates rocks are characterized by intermediate concentrations. The process of lateritization during bauxite formation contributes to increase the ratio Th/U, which is generally more than 4 (Adams and Richardson, 1960).

Bayer process is used for refining bauxite to smelting grade alumina, the aluminium precursor: it involves the digestion of crushed bauxite in a concentrated sodium hydroxide solution at temperatures up to 270°C. Under these conditions, the majority of the species containing aluminium is dissolved in solution in the ore, while the insoluble residues are filtered making a solid waste called “red mud”. The alumina is obtained by the hydroxide solution after the processes of precipitation and calcination (Hind et al., 1999). Finally, by using the Hall-Heroult electrolytic process, alumina is reduced to aluminium metal.

The fact that thorium and radium in an hydroxide medium are practically insoluble (Somlai et al., 2008) could disturb especially the secular equilibrium of the uranium chain, as it has been observed in some measurements (Pontikes et al., 2006). However, some “results indicate that the chemical processing of the bauxite ore has not significant consequences in the secular equilibrium of either the uranium or thorium series” (Cooper et al., 1995). In the process of extracting alumina from bauxite, over 70% of the thorium and radium are concentrated in the red mud (Adams and Richardson, 1960).

In 2009 the worldwide production of bauxite and alumina was  $199 \cdot 10^9$  kg and  $123 \cdot 10^9$  kg respectively. Considering that the worldwide ratio bauxite/alumina, averaged in the period 1968-2009, is  $2.7 \pm 0.1$ , we expect that  $1.7 \pm 0.1$  kg of red mud is generated per kg of alumina (USGS Data Series 140). By assuming that at least 70% of the radioisotopes in bauxite accumulate in the red mud, the increasing factor of radioactivity content in the red mud varies in a range of 1.1 and 1.6. Using these estimated enrichments for bauxite we encompass a large portion of the radium and thorium activities of the red mud reported in literature (Table 2).

Based on recent statistics, more than  $70 \cdot 10^9$  kg of red mud is discharged annually in the world: it constitutes the most important disposal problem of the aluminium industry. The mud is highly basic (pH > 10) and its storage on huge area can cause environmental pollution, soil basification, paludification, surface water and groundwater pollution as well as resource pollution. The safe treatment of this NORM is an increasing social problem. Moreover, a considerable attention has been given to additional uses of bauxite wastes: they include metallurgical extractions, building materials productions and the development of new ceramics and catalytic materials. Gamma-ray spectrometers are able to process thousands of measurements in order to perform environmental monitoring and to control the recycled by-products. The MCA\_Rad system described in section 3 could be extremely helpful for processing these measurements by significantly diminishing manpower costs.

**Table 2.** Activity concentration in red mud reported in the literature: in a) the range indicated correspond to the maximum and minimum value measured for different samples and in b) the

uncertainties of measurement results. The activities quoted are assumed equal to  $^{228}\text{Ac}$  in 1), equal to  $^{228}\text{Th}$  in 2) and equal to  $^{238}\text{U}$  in 3).

Authors of the study	Country	Activities (Bq kg <sup>-1</sup> )	
		$^{226}\text{Ra}$	$^{232}\text{Th}$
Papatheodorou et al., 2005 <sup>a)</sup>	Greece	13 – 185	15 – 412
Philipsborn and Kuhnast 1992 <sup>b) 1)</sup>	Germany	122 ± 18	183 ± 33
Pinnock, 1991 <sup>a)</sup>	Jamaica	370 – 1047	328 – 350
Somlai et al., 2008 <sup>a)</sup>	Hungary	225 – 568	219 – 392
Akinci and Artir, 2008 <sup>b)</sup>	Turkey	210 ± 6	539 ± 18
Jobbágy et al., 2009 <sup>a)</sup>	Hungary	102 – 700	87 – 545
Cooper et al., 1995 <sup>b) 2)</sup>	Australia	310 ± 20	1350 ± 40
Turhan et al., 2011 <sup>a)</sup>	Turkey	128 – 285	342 – 357
Pontikes et al., 2006 <sup>b) 2)</sup>	Greece	379 ± 43	472 ± 23
Beretka and Mathew, 1985	Australia	326	1129
Georgescu et al., 2004	Romania	212	248
Döring et al., 2007 <sup>b)</sup>	Germany	190 ± 30	380 ± 50
Ruyters et al., 2011 <sup>3)</sup>	Belgium	550	640

### *Mineral sand and downstream productions*

The extraction of mineral sand ore is important for the production of heavy minerals (with densities heavier than 2.8 g cm<sup>-3</sup>) like titanium, tin and zirconium bearing minerals and rare earth elements<sup>4</sup> (REEs). The deposits of hard minerals, which do not undergo erosion and transport processes, mainly occur when they have been concentrated by marine, alluvial and/or wind processes. These placer deposits can be found also in vein deposits, mostly disseminated in alkaline intrusions in hard rocks. The radioactivity concentration of mineral sand can be of the order of a few hundreds Bq kg<sup>-1</sup>, depending on the placer geology. In heavy minerals we can often find high content of radioactivity, sometimes of the order of hundreds kBq kg<sup>-1</sup>.

The process involved in heavy mineral extraction includes two main phases of separation. The first phase separates the heavy mineral concentration, by using either dry operation or dredging of the slurried ore: this produces high amount of residues with a radionuclide concentration of the same order of mineral sand (Paschoa, 2008). During the second phase, the heavy mineral concentration is further separated mainly by combining dry magnetic and electrostatic processes. This allows the concentration of various minerals, such as titanium bearing minerals (ilmenite, leucoxene, rutile), zircon bearing minerals (zircon, baddeleyite) and REEs bearing minerals (monaxite, zenotime). The products of this second phase generally show a high content of radioisotopes.

Titanium bearing minerals are used mainly to produce TiO<sub>2</sub> pigment. The radioactivity concentration in these minerals varies in rutile (400 - 2900 Bq kg<sup>-1</sup> Th and 250 – 500 Bq kg<sup>-1</sup> U) and ilmenite (400 – 4100 Bq kg<sup>-1</sup> Th and 250 – 750 Bq kg<sup>-1</sup> U) (IAEA\_2003b; Timmermans and van der Sten, 1996; McNulty, 2007). The higher production efficiency is obtained by rutile: it is directly processed through the chloride route producing TiO<sub>2</sub> pigment/waste with a ratio of 5/1 (USGS MCS, 1996). Since the radioisotopes follow the liquid waste stream, the radioactivity concentration in the waste is very high due to the severe mass reduction.

<sup>4</sup> REEs contain 16 chemical elements, including those with atomic numbers 57 (lanthanum) through 71 (lutetium), as well as yttrium (atomic number 39), which has similar chemical properties.

Ilmenite requires a pre-processing in order to produce synthetic rutile: the product/waste ratio is 10/7. The synthetic rutile is further processed through the chloride route in order to produce TiO<sub>2</sub> pigment with a product/waste ratio of 5/6, showing a light enhancement of radioactivity concentration in waste of ilmenite processing ([IAEA\\_2003b](#)).

In TiO<sub>2</sub> pigment production the most relevant NORM are made by the chloride treatment of rutile. The worldwide production of TiO<sub>2</sub> in 2010 was about  $5.7 \cdot 10^9$  kg when the mineral extraction ratio is 1/10 for rutile/ilmenite ([USGS MCS, 2011](#); [IAEA\\_2003b](#)): about 2% of the total waste which has been generated can show a strong enhancement in radioactivity concentration.

The most common zirconium bearing minerals are zircon and baddeleyite: in 2010 the world extraction of these minerals was about  $1.2 \cdot 10^9$  kg ([USGS MCS, 2011](#)). Mineral sands containing zircon are commonly used in ceramic and refractory industries. The zircon crystal lattice host uranium and thorium: their activities in zircon bearing minerals are in the range of 1-5 kBq kg<sup>-1</sup> for U and of 0.5-1 kBq kg<sup>-1</sup> for Th respectively ([Righi et al., 2005](#)).

The manufacture of zirconia is mainly performed by fusion of feedstock with coke near to zirconium molten temperatures. It causes the dissociation of mineral in ZrO<sub>2</sub> and SiO<sub>2</sub>: during the fusion U and Th end up almost at the same concentration in zircon product, while <sup>226</sup>Ra tends to end up in silica, causing the disequilibrium of U decay chain. The subsequent caustic fusion process at 600°C increases the purity of zirconia. During the chemical dissolution, zircon crystal structure is destroyed, yielding nearly 100% of uranium recovery in the form of sodium uranate ([Brown and Costa, 1972](#)). The performances of MCA\_Rad system completely fit the need of measuring radioactivity content in this kind of NORM.

The main minerals used as sources of REEs can be extracted by placer deposits (monazite and xenotime) and by hard rocks (bastnaesite, coperite and pyrochlore). Monazite minerals are characterized by high activity concentration of U (25-75 kBq kg<sup>-1</sup>) and Th (41-575 kBq kg<sup>-1</sup>). The chemical attack of the mineral based on NaOH separates sodium phosphate from a mixture called "cake I", which is rich in heavy minerals. Cake I is further filtered, given that it yields a concentration of rare earth chlorides and a mixture called "cake II" containing most of thorium and uranium originally present in monazite feedstock ([Paschoa, 1997](#)). The decay chain of U and Th are not in secular equilibrium in cake II: thorium precipitates while radium remains in solution. The latter can reach very high activities (7 MBq kg<sup>-1</sup> and 10 MBq kg<sup>-1</sup> for <sup>226</sup>Ra and <sup>228</sup>Ra respectively) ([Paschoa, 2008](#)). In 2010, the extraction of monazite has been  $1.3 \cdot 10^8$  kg ([USGS MCS, 2011](#)) and its processing has made 10% of cake II waste ([Paschoa, 1993](#)). This large amount of highly enhanced radioactivity NORM requires scrupulous monitoring and control.

### ***2.3 Industrial minerals extraction and processing***

#### *Phosphate fertilizer industry*

The main phosphate-rock (phosphorite) deposits are both of igneous and sedimentary origin and they are part of the apatite group. They are commonly encountered as fluorapatite and francolite respectively. A specific characteristic of phosphate rocks consists in a low ratio Th/U, in general less than 0.5, which is mainly due to relative high concentrations of uranium commonly between 370 and 2470 Bq kg<sup>-1</sup> and sometimes higher than 12.35 kBq kg<sup>-1</sup>. Uranium and thorium decay chains are generally found to be in secular equilibrium ([Menzel, 1968](#)).

Phosphorite is mainly processed through the so-called "wet process", which includes chemical treatments, mostly by using sulfuric acid: the products are phosphoric acid (PA) and an insoluble calcium sulfate salt called phosphogypsum (PG), with a ratio PG/PA = 5 ([Tayibi et al., 2009](#)). PA and PG are usually separated by filtration and reactor off-gas and vapors. These

processes concentrate the trace elements in PA or PG in various amounts causing secular disequilibrium in U and Th decay chains. In PG is found approximately 80 – 90% of the  $^{226}\text{Ra}$  along with a high content of  $^{210}\text{Pb}$  and  $^{210}\text{Po}$  (Carvalho, 1995; Beddow et al., 2006), as a consequence of the similar chemistry (Guimond and Hardin, 1989; Beddow et al., 2006). About 80 – 85% of the uranium (Poole et al., 1995; Beddow et al., 2006) and about 70% of thorium (Tayibi et al., 2009) concentrate in PA. As a consequence of these processes, we expect a relevant enhancement of U concentration in PA and an abundance of Ra in PG comparable with that in phosphate-ore (Table 3). The high production of phosphogypsum requires constant controls in order to make a secure stockage and reutilization of such material. These controls must be extended to PA and phosphate fertilizers: the MCA\_Rad system described in the next section has been designed to deal with automatic gamma ray measurements on large amounts of PA and PG samples.

**Table 3.** Studies on activities of phosphate rock (PR) and phosphogypsum (PG) in different countries.

Authors of the study	Country	$^{238}\text{U}$ (Bq kg <sup>-1</sup> )		$^{226}\text{Ra}$ (Bq kg <sup>-1</sup> )	
		PR	PG	PR	PG
Mazilli et al., 2000	Brazil	-	-	130 - 1445	93 - 729
Silva et al., 2001	Brazil	434 - 1128	66 - 140	407 - 1121	228 - 702
Saueia et al., 2005	Brazil	14 - 638	<2 - 61	53 - 723	24 - 700
Santos et al., 2006	Brazil	102 - 1642	32 - 69	239 - 862	307 - 1251
Saueia et al., 2006	Brazil	158 - 1868	40 - 58	139 - 1518	122 - 940
El Afifi et al., 2009	Egypt	916	140	890	459
Azouazi et al., 2001	Morocco	2100 - 2450	-	1850 - 2320	1420
Carvalho, 1995	Portugal	1003	26 - 156	1406	950 - 1043
Hull and Burnett, 1996	USA (Central Florida)	848 - 1980	45 - 368	882 - 1980	505 - 1353
	USA (Northern Florida)	242 - 982	23 - 452	230 - 883	270 - 598

### 3. MCA\_Rad system

An accurate radiological characterization of NORM requires careful investigation on a case-by-case basis. Indeed the NORM issue shows high levels of complexity mainly due to the huge amount of worldwide waste production perturbed by the different geochemical composition of raw materials and the effective concentration of a wide range of industrial processes. Most of current studies show that determining the content of  $^{226}\text{Ra}$ ,  $^{228}\text{Ra}$  and  $^{40}\text{K}$  radioisotopes in NORM is mandatory for radiation protection. High resolution gamma-ray spectrometry is a frequently used non-destructive technique, which provides an accurate identification and quantitative determination of such radioisotopes.

A strategic approach to the NORM issue consists in constructing systematic monitoring programmes. However, this approach is often limited by funding and manpower capacities of a laboratory. Indeed, when a laboratory deals with random measurements, the main costs are determined by the instrument investment programme; instead, for a routine monitoring program the substantial costs are due to the manpower involved. The MCA\_Rad system introduces an innovative configuration of a laboratory high-resolution gamma-ray spectrometer featured with a complete automation measurement process. Two HPGc detectors allow to achieve both good statistical accuracy in a short time and *ad hoc* approach to low-background shielding construction



design. This self-constructed instrument drastically minimizes measurement and manpower costs.

### 3.1 Set-up design and automation

The core of the MCA\_Rad system is made of two 60% relative efficiency coaxial p-type HPGe gamma-ray detectors, which possess an energy resolution of about 1.9 keV at 1332.5 keV ( $^{60}\text{Co}$ ). Both detectors are controlled by individual integrated gamma spectrometers for the digital signal processing. The new cooling technology, which employs mechanical coolers, allows to simplify the management of the system. The detectors are accurately shielded and positioned facing each other 5 cm apart (**Fig. 1a**).

The background spectrum of a gamma ray spectrometer is mainly due to the combination of cosmic radiation, environmental gamma radiation and the radioactivity produced by radioimpurities both in the shielding materials and in the detector. In order to effectively reduce the environmental gamma radiation, an adequate shielding construction is needed.

In the MCA\_Rad a 10 cm thick lead house shields the detector assembly, leaving an inner volume around the detectors of about 10 dm<sup>3</sup> (**Fig.1a** and **1b**). The lead used as shielding material adds some extra background due to the presence of  $^{210}\text{Pb}$ , produced by  $^{238}\text{U}$  decay chain. This isotope, which has an half life of 22.3 years, is revealed by a gamma energy of 46.5 keV and a *bremsstrahlung continuum* from beta decay of its daughter  $^{210}\text{Bi}$  extending from low energy up to 1162 keV. Furthermore, when a gamma ray strikes the lead surface, characteristic lead X-rays may escape and hit the detector (**Smith et al., 2008**).

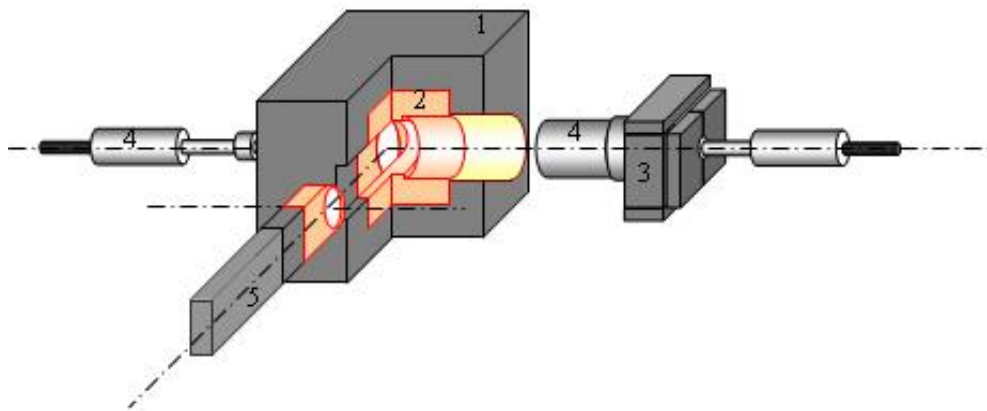


**Figure 1a.** Schematic design of the MCA\_Rad system. 1) The main lead shielding construction (20 cm x 25 cm x 20 cm). 2) The core copper shielding (10 cm x 15 cm x 10 cm). 3) Rear lead shielding construction. 4) HPGe semiconductor detectors. 5) The mechanical sample changer.

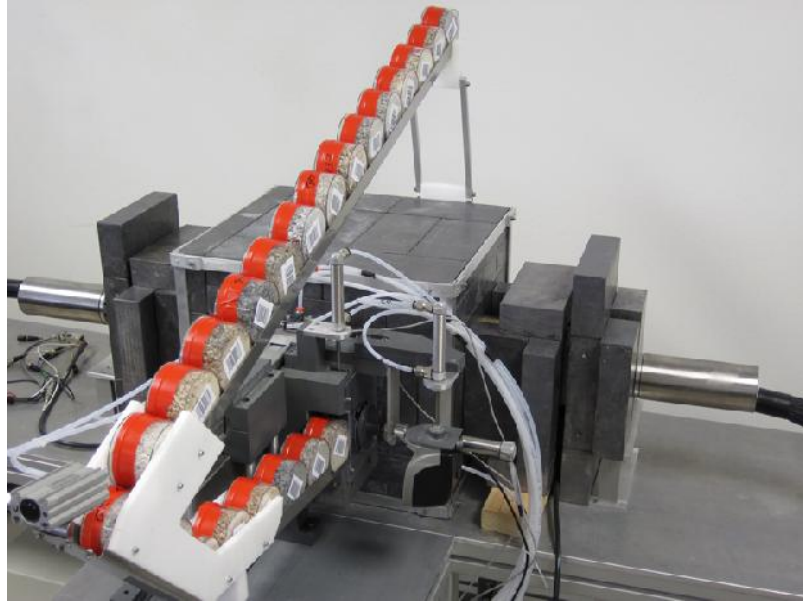


**Figure 1b.** View of the MCA\_Rad system.

The inner volume is occupied by 10 cm thick oxygen free copper house, which allows to host the sample under investigation. In order to reduce the X-rays coming from the sample, the end-cup windows of the detectors is further shielded with a tungsten alloy sheet of 0.6 mm. A 10 mm thick bronze cylinders and walls of about 10 cm of lead are also shielding the rear part of the system. [Fig.1a](#) and [1b](#)). The final intrinsic background is reduced by two order of magnitude compared to other unshielded detectors (see [Fig. 2](#)).

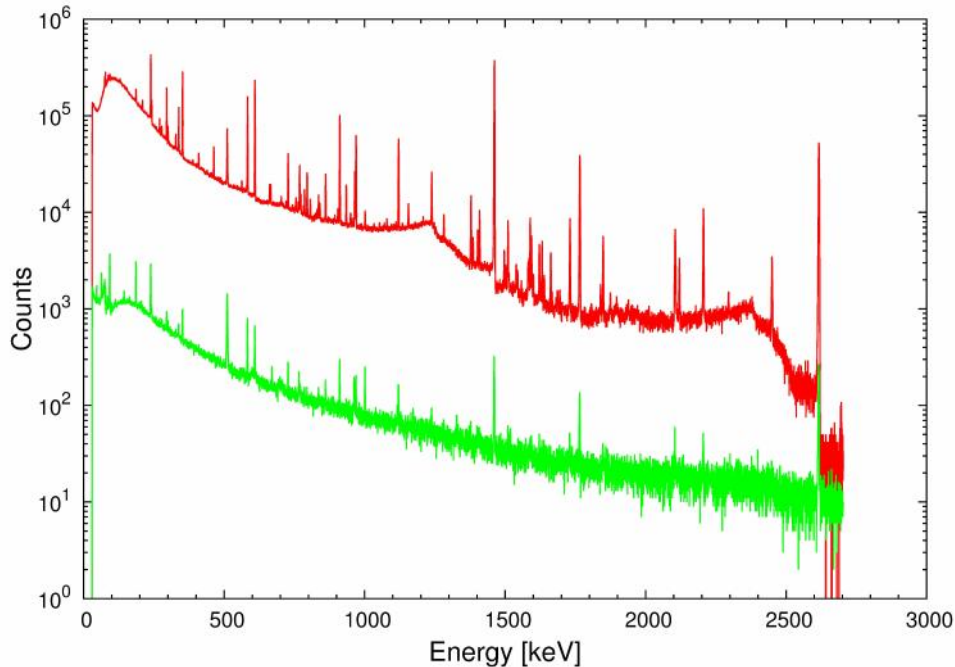


**Figure 2.** The MCA\_Rad system background spectra (acquisition live time 100 h) with (green) and without (red) shielding. Spectra are obtained by summing the single detector background after rebinning with 0.33 keV/channel.

As a good practice of gamma-ray spectrometry analysis, information concerning background spectra is required both to detect any potential residual contaminations and for background corrections. A background measurement with acquisition time of several days is

performed regularly. The final sensitivity of the measurements can be evaluated by using the detection limit ( $L_D$ ) described in (Currie, 1986), assuming the Gaussian probability distribution of the number of counts in the background (B) and rejecting the data not included in a range of  $1.645\sigma$  (95% confidence level):

$$L_D = 2.71 + 4.65\sqrt{B} \approx 4.65\sqrt{B} \quad (1)$$

where the approximation is admitted for high number of counts. The minimum detectable activity (MDA) for the background is calculated using the  $L_D$ , according to the formula:

$$MDA = \frac{L_D}{\varepsilon I_\gamma t} \quad (2)$$

where  $\varepsilon$  is the absolute efficiency (calculated as described below),  $I_\gamma$  is the gamma line intensity and  $t$  is the acquisition live time. In Table 4 we report the typical one hour acquisition live time background counts and the sensitivity of the measurement expressed by  $L_D$  and MDA for the main gamma lines used to calculate the radionuclide concentrations in NORM.

**Table 4.** MCA\_Rad system characterization of typical one hour (live time) background (B in counts) for the most important energies and the corresponding detection limit  $L_D$  and minimum detectable activity (MDA) (Currie, 1986) for 95% confidence interval (CI).

Parent isotope	Daughter isotope	Energy (keV)	B (counts)	$L_D$ (counts)	MDA (Bq)
$^{238}\text{U}$	$^{234\text{m}}\text{Pa}$	1001.0	$8 \pm 1$	21	22.16
	$^{214}\text{Pb}$	351.9	$31 \pm 2$	49	0.50
	$^{214}\text{Bi}$	609.3	$44 \pm 1$	32	0.49
$^{232}\text{Th}$	$^{228}\text{Ac}$	911.2	$27 \pm 1$	27	0.94
	$^{212}\text{Pb}$	238.6	$100 \pm 2$	62	0.46
	$^{212}\text{Bi}$	727.3	$10 \pm 1$	31	3.00
	$^{208}\text{Tl}$	583.2	$42 \pm 1$	33	0.71
$^{40}\text{K}$	$^{40}\text{K}$	1460.8	$151 \pm 1$	19	5.53

The sample material is contained in a cylindrical polycarbonate box of 75 mm in diameter, 45 mm in height and  $180 \text{ cm}^3$  of useful volume, labeled by a barcode. Up to 24 samples can be charged in a slider moving by gravity and further introduced at the inner chamber through an automatic “arm” made of copper, lead and plastic closing the lateral hole of the housing (Fig. 1b). The mechanical automation consists on a barcode scanner and a set of compressed air driven pistons. This mechanism not only makes the sample identification possible, but is also able to introduce/expel the samples. All operations, including measurements, are controlled by a PC by means of a dedicated software.

The program receives by the operator an input file with relevant information about the slot of samples: acquisition live time, spectra file name, sample weight, sample description and barcode. The procedure is repeated until the barcode reader detects samples. A new batch command file is generated to be successively employed in spectrum analysis. In order to complete the automation of the MCA\_Rad system, a user-friendly software has been developed for spectra analysis. The code adopts ANSI No. 42.14, 1999 standard specification for the peak analysis.

### 3.2 Calibration and data analysis

For each measurement, the final spectrum is obtained by adding, after rebinning, the two simultaneously measured spectra: for this purpose an accurate energetic calibration of the system, along with a periodical check, is required. When a shift larger than 0.5 keV is observed, the energy calibration procedure is repeated.

The absolute photopeak efficiency ( $\varepsilon_p$ ) for the MCA\_Rad system has been determined by using standard point sources method, and producing the calibration curve. Two low activity point sources with complex decay schemes are used (**DeFelice et al., 2006**): a certified  $^{152}\text{Eu}$  source, with an activity of 6.56 kBq in 1995, known with an uncertainty of 1.5% and a  $^{56}\text{Co}$  home made source, that has been normalized relative to  $^{152}\text{Eu}$  by calculating the activity of the 846.8 keV ( $^{56}\text{Co}$ ) gamma line. The  $^{56}\text{Co}$  source is used in order to extend the efficiency calibration for gamma energies up to 3000 keV.

The spectra obtained are corrected for: 1) coincidence summing,  $C_{CS}$ , on each individual detector, produced by the complex decay scheme of the sources, 2) differences between the geometry of the point sources and the sample shape,  $C_G$  and 3) self-attenuation,  $C_A$ , of gamma-rays within the sample volume.

The correction due to coincidence summing is studied by following the method described in (**DeFelice et al., 2000**) and obtained as a relationship between the single total efficiency ( $\varepsilon_t$ ), the single apparent absolute photopeak efficiency ( $\varepsilon_p^{app}$ ) and isotope decay data. The single total efficiency is obtained by estimating the peak-to-total ratio ( $P/T$ ) using the empirical approach described by (**Cesana and Ferrani, 1989**) and recalling the relationship  $\varepsilon_p^{app} / \varepsilon_t = P/T$ . The decay coefficients for  $^{152}\text{Eu}$  were calculated from decay data taken from **Monographie BIPM-5, 2004**, while those for  $^{56}\text{Co}$  were taken from **Tomarchio and Rizzo, 2011** and **Dryák and Kovář, 2009**. Finally, the absolute efficiency,  $\varepsilon_p(E)$ , of the MCA\_Rad system is given by the sum of single HPGe detector contribution corresponding to the characteristic gamma energies ( $E_i$ ) of the standard calibration sources used.

$$\varepsilon_p(E_i) = \varepsilon_p^{app}(E_i)C_{CS}(E_i) \quad (3)$$

Then the absolute efficiency is obtained for the energetic range from 200 keV to 3000 keV by fitting them using the function given by **Knoll, 1999** (**Fig. 3**):

$$\varepsilon(\%) = (b_0 E / E_0)^{b_1} + b_2 \exp(-b_3 E / E_0) + b_4 \exp(-b_5 E / E_0) \quad (4)$$

where  $E$  (keV) is the gamma-ray energy;  $E_0 = 1$  keV is introduced to make dimensionless the argument of the exponential dimensionless and  $b_i$  are the fitting parameters (where  $b_0 = 1.38$ ,  $b_1 = 1.41$ ,  $b_2 = 22.97$ ,  $b_3 = 5.43$ ,  $b_4 = 6.61$  and  $b_5 = 0.44$ ).

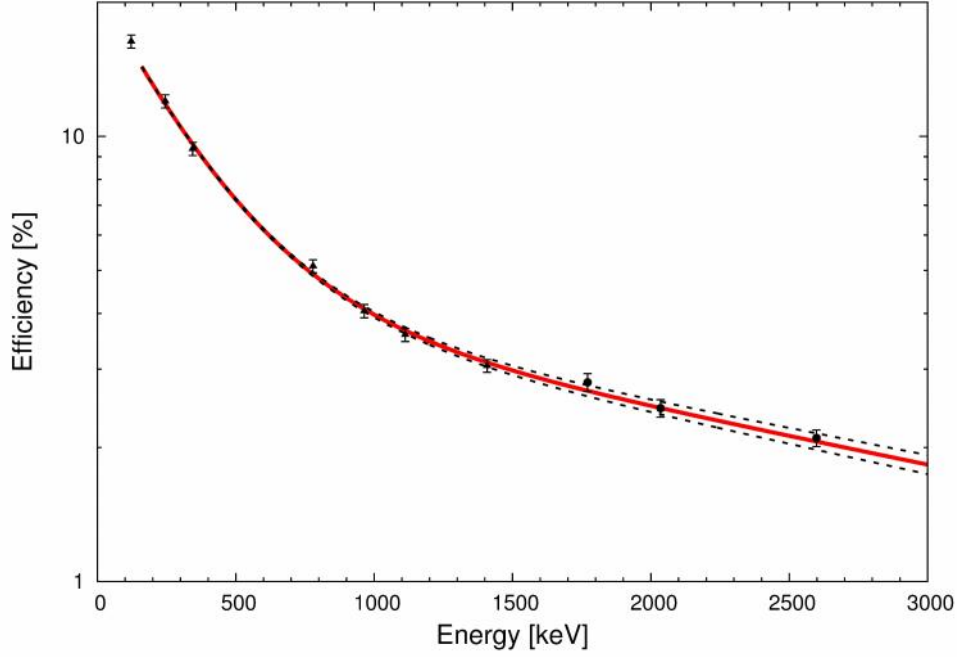


**Figure 3.** Absolute efficiency curve of MCA\_Rad system. It is obtained by fitting  $^{152}\text{Eu}$  (triangle) and  $^{56}\text{Co}$  (circle) energies with Eq. 2 performing the best fit (in red). Dashed curves represent  $\pm$  one sigma uncertainty interval.

The effect of volume geometry can be described in terms of the effective solid angle developed analytically by [Moens et al., 1981](#) within less than 2% of uncertainty between numerical and experimental calculations. The geometrical factor ([Fig. 4](#)) for MCA\_Rad system is deduced from a set of measurements using a  $^{56}\text{Co}$  and  $^{57}\text{Co}$  point sources placed at different radial distances (center, middle and lateral) from the detector axis at different planes, reconstructing the sample geometry using the formula:

$$C_G(E_i) = \frac{\bar{\Omega}_x}{\Omega_{ref}} \approx \frac{1}{R_{ref}(E_i)} \sum_{j=1}^N \frac{[R_x(E_i)]_j}{N} \quad (5)$$

where  $R_x(E_i)$  is the net count rate in the standard spectrum collected in different positions (j) and  $R_{ref}(E_i)$  is the net count rate in the standard spectrum collected in the reference positions (center). The geometrical correction factor is obtained as a function of energy by fitting a third order polynomial as a function of energy ([Fig. 4](#)):

$$C_G(E) = \sum_{i=0}^4 a_i \left( \frac{E}{E_0} \right)^i \quad (6)$$

where  $E_0 = 1$  keV is introduced to make the argument dimensionless and  $a_i$  are the fitting coefficients ( $a_0 = 0.8678$ ,  $a_1 = 0.1098$ ,  $a_2 = -0.0541$ ,  $a_3 = 0.0077$ ).

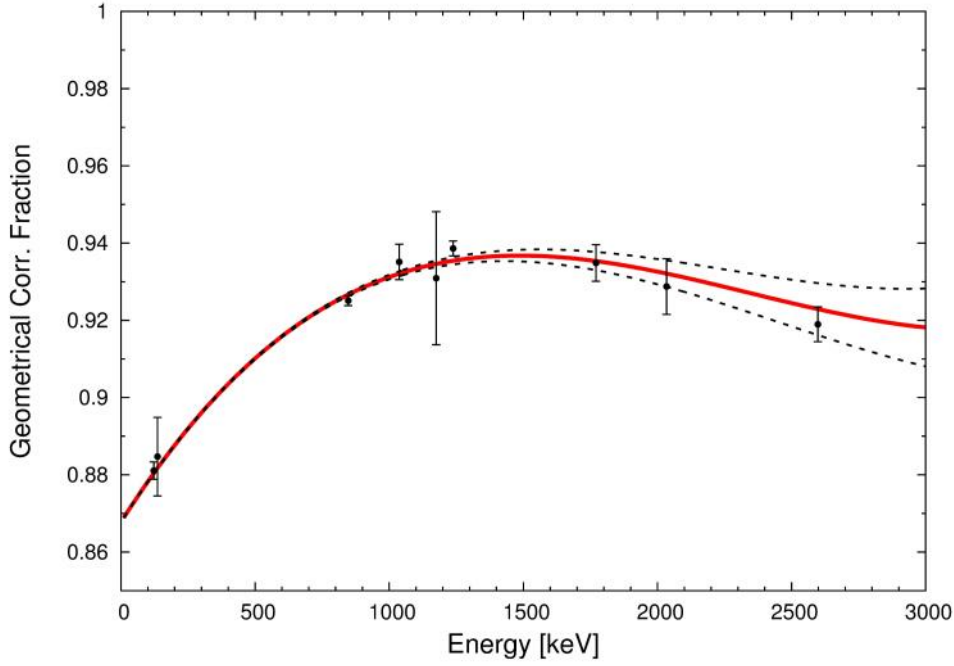


**Figure 4.** The geometrical correction factor due to differences between calibration (point source) and measurement geometry (cylinder of 75 mm of diameter and 45 mm of height), which is obtained by fitting nine photopeaks of  $^{56}\text{Co}$  and  $^{57}\text{Co}$  with a third order polynomial. Dashed curves represent  $\pm$  one sigma uncertainty interval.

The gamma-ray attenuation correction  $C_{SA}$  is calculated for different kind of samples taking into account their differences in density by a simplified expression deduced by [Cutshall et al, 1983](#) and [Bolivar et al, 1997](#):

$$C_{SA} = \frac{1 - \exp(-\mu_1 t)}{\mu_1 t} \quad (7)$$

where  $\mu_1 = \mu\rho$  ( $\text{cm}^{-1}$ ) is the linear mass attenuation coefficient,  $\mu$  ( $\text{cm}^2 \text{g}^{-1}$ ) is the mass attenuation coefficient,  $\rho$  ( $\text{g cm}^{-3}$ ) is the sample density and  $t$  (cm) is the sample effective thickness (which in our case is the half thickness of the sample container). The mass attenuation coefficient is strongly  $Z$  dependent in the energy range below few hundred keV while for higher energies the trend is smoother and it depends mainly on energy. These features can be used, since NORM characterization, especially concerning  $^{226}\text{Ra}$ ,  $^{228}\text{Ra}$  and  $^{40}\text{K}$ , requires the investigation of gamma-rays with energies higher than hundreds keV. We can parameterize the mass attenuation coefficient as a function of energy. We used XCOM 3.1 database, which is available on-line and developed by the Nuclear Institute of Standards and Technology (NIST). It is calculated by using For various rocks forming minerals, the average mass attenuation coefficient was deduced with a standard deviation of less than 2% in the energetic range 200 – 3000 keV.

$$\bar{\mu}(E) = \sum_{i=0}^2 a_i [\ln(E)]^i \quad (8)$$

where  $a_i$  ( $a_0 = 0.5593$ ,  $a_1 = -0.1128$ ,  $a_2 = 0.0590$ ) are coefficients determined by fitting this function with a reduced chi-square of  $\chi^2_\nu = 1.12$ . Finally the self attenuation correction factor was given as a function of gamma-ray energy and sample density through the relationship:

$$C_{SA}(E, \rho_s) = \exp[b_0 + b_1 \ln(E) + b_2 \ln(E)^2] \rho_s \quad (9)$$

where  $b_i$  ( $b_0 = 1.2609$ ,  $b_1 = -0.2547$ ,  $b_2 = 0.0134$ ) are coefficients determined by fitting this function.

The uncertainty budget for the calibration procedure is reported in **table 5**. Considering the uncertainties due to geometrical and self-attenuation correction factors as systematic errors, the overall uncertainty about the absolute efficiency of the MCA\_Rad system is estimated to be less than 5%.

**Table 5.** Uncertainty budget for absolute efficiency determination.

Uncertainty source	Relative uncertainty (%)
Certified standard source uncertainty	1.5*
Coincidence summing correction factor	< 2
Geometrical correction factor	< 2
Self attenuation correction factor	< 2

\* 95% of confidence level.

### 3.3 Measurement of reference materials

The applicability of the MCA\_Rad system as well as the method quality control was cross checked using certified reference materials containing concentrations comparable to NORM values. Three reference materials certified within 95% of confidence level prepared in powder matrix (240 mesh) containing  $^{238}\text{U}$  (IAEA RGU-1)  $4940 \pm 30 \text{ Bq kg}^{-1}$ ,  $^{232}\text{Th}$  (IAEA RGTh-1)  $3250 \pm 90 \text{ Bq kg}^{-1}$  in secular equilibrium and  $^{40}\text{K}$  (IAEA RGK-1)  $14000 \pm 400 \text{ Bq kg}^{-1}$  are used. The sample boxes were filled with the reference materials, after were dried at  $60^\circ\text{C}$  temperature, hermetically sealed and then left undisturbed for at least 3 weeks in order to establish radioactive equilibrium in  $^{226}\text{Ra}$  decay chain segment prior to be measured.

In **Table 6** we report the specific activity calculated for the principal gamma lines used to estimate the isotopes of uranium and thorium decay chain and for potassium using the formula:

$$A (\text{Bq} / \text{kg}) = \frac{R}{\varepsilon I_\gamma m} C_{SA} C_G C_{CS}^* \quad (10)$$

where  $R$  is the measured count rate (background corrected),  $\varepsilon$  is the absolute efficiency,  $I_\gamma$  is the gamma line intensity,  $m$  is the mass of the sample,  $C_{SA}$  is the correction factors for self-absorption,  $C_G$  is the geometrical correction factor and  $C_{CS}^*$  is the coincidence summing correction factor (calculated using the same approach as described above for the specific decay chains of the uranium and thorium). The results have an overall relative discrepancy of less than 5% among certified central values within the reported uncertainty.

**Table 6.** In the sixth column we report the activity concentrations (in  $\text{Bq kg}^{-1}$ ) calculated for the main energetic lines used for  $^{238}\text{U}$  and  $^{232}\text{Th}$  decay chains and for  $^{40}\text{K}$  together with respective statistical uncertainties. The reference material activities certificated by IAEA are shown in seventh column. The correction coefficients  $C_{CS}^*$  and  $C_{SA}$  are referred to coincidence summing and self absorption respectively.

Parent Isotope	Daughter Isotope	E (keV)	C <sub>CS</sub> *	C <sub>SA</sub>	Activity (Bq kg <sup>-1</sup> )	Certified Reference Material Activity (Bq kg <sup>-1</sup> )
<sup>238</sup> U	<sup>234m</sup> Pa	1001.0	1.000	1.24	4875 ± 48	4940 ± 30
	<sup>214</sup> Bi	609.3	1.190	1.32	4872 ± 4	
	<sup>214</sup> Pb	351.9	1.002	1.42	4773 ± 3	
<sup>232</sup> Th	<sup>228</sup> Ac	911.2	1.024	1.24	3092 ± 4	3250 ± 90
	<sup>212</sup> Pb	238.6	0.990	1.48	3246 ± 2	
	<sup>212</sup> Bi	727.3	1.056	1.27	3389 ± 9	
	<sup>208</sup> Tl	583.2	1.298	1.31	3342 ± 4	
<sup>40</sup> K	-	1460.8	-	1.21	14274 ± 71	14000 ± 400

#### 4. Conclusions

We presented a summary of the main categories of non-nuclear industries together with the levels of activity concentration in feeding raw materials, products, by-products/waste and the possible enhancement mechanisms. The main chemical and physical processes that disturb the secular equilibrium of uranium and thorium decay chains have been reported. The degree of radioactivity enhancement is studied along with the radioactivity level in feeding raw material and the industrial process involved. A refined estimation of radioactivity concentrations of <sup>226</sup>Ra, <sup>228</sup>Ra and <sup>40</sup>K in NORM is almost impossible in such a wide range of industrial activities: the strategy that we propose consist in a systematic monitoring and continuous checking based on high-resolution gamma-ray spectroscopy.

For this purpose an innovative approach to the configuration of a laboratory low background high-resolution gamma-ray spectrometer, MCA\_Rad system, was developed and featured with fully automated measurement processes. It presents the following advantages.

- The new design of lead and copper shielding configuration allowed to reach a background reduction of two order of magnitude respect to laboratory radioactivity.
- A severe lowering of manpower cost is obtained by a fully automation system which permits to measure up to 24 samples without any human attendance.
- The two HPGe detectors offer higher detection efficiency: confronting the MDA of the system with typical NORM values, it can be deduced that measurements in less than one hour are realized with uncertainties of less than 5%.
- Accurate measurements are performed on small sample volume (180 cc) with a reduction of material transport costs.
- A user-friendly software has been developed in order to analyze a high number of spectra, possibly with automatic procedure and customized output.

An empirical efficiency calibration method using multi-gamma standard point sources is discussed. The correction factors affecting the measured spectra (coincidence summing, sample shape, sample gamma-ray self-attenuation) are given with respective procedures. As a result of this procedure the absolute efficiency is estimated to have an overall uncertainty of less than 5%. A test of the applicability of the instrument as well as the method quality control using certified reference materials showed an overall relative discrepancy of less than 5% among certified central values within the reported uncertainty.

We, therefore, conclude that the MCA\_Rad system shows efficacy in the face of the NORM issue, by increasing the capacities of a laboratory and offering accurate results with a reduction of manpower costs.



**Acknowledgement**

We are grateful for useful comments and discussions to P. Altair, M. Baloncini, E. Bellotti, L. Carmignani, L. Casini, V. Chubakov, T. Colonna, M. Gambaccini, Y. Huan, W. F. McDonough, G. Oggiano, R. L. Rudnick and R. Vannucci.

This work was partially supported by INFN (Italy) and by Fondazione Cassa di Risparmio di Padova e Rovigo.

## References

- Abo-Elmagd M., Soliman H.A., Salman Kh.A., El-Masry N.M., 2010. Radiological hazards of TENORM in the wasted petroleum pipes. *Journal of Environmental Radioactivity* 101, 51–54.
- ACAA, American Coal Ash Association, 2003. “Fly Ash facts for highway engineers”. Federal highway association report FHWA-IF-03-019.
- Adams J.A.S., and Richardson, K.A. 1960. Thorium, Uranium and Zirconium concentration in Bauxite. *Economic Geology* 55, 1653–1675.
- Akinci A. and Artir R., 2008. Characterization of trace elements and radionuclides and their risk assessment in red mud. *Materials Characterization* 59, 417–421.
- Al-Masri M.S., Suman H., 2003. NORM waste management in the oil and gas industry: The Syrian experience. *Journal of Radioanalytical and Nuclear Chemistry* 256, 159–162.
- Al-Saleh F.S., Al-Harshan G.A., 2008. Measurements of radiation level in petroleum products and wastes in Riyadh City Refinery. *Journal of Environmental Radioactivity* 99, 1026–1031.
- ANSI No.42.14, 1999. American national standard for calibration and use of germanium spectrometers for the measurement of gamma-ray emission rates of radionuclides.
- Azouazi M., Ouahidi Y., Fakhi S., Andres Y., Abbe J.Ch., Benmansour M., 2001. Natural radioactivity in phosphates, phosphogypsum and natural waters in Morocco. *Journal of Environmental Radioactivity* 54, 231–242.
- Bakr W.F., 2010. Assessment of the radiological impact of oil refining industry. *Journal of Environmental Radioactivity* 101, 237–243.
- Beck H. L., 1989. Radiation Exposures Due To Fossil Fuel Combustion. *International Journal of Radiation Applied Instruments, Part C. Radiation Physics Chemistry* 34, 285–293.
- Beddow H., Black S., Read D., 2006. Naturally occurring radioactive material (NORM) from a former phosphoric acid processing plant. *Journal of Environmental Radioactivity* 86, 289–312.
- Beretka J., Mathew P. J., 1983. Natural Radioactivity of Australian building material wastes and by-products. *Health Physics* 48, 87–95.
- Bolivar J.P., Garcia-Leon M., Garcia-Tenorio R., 1997. On Self-attenuation Corrections in Gamma-ray Spectrometry. *Appl. Radiat. Isot.* 48, 1125–1126.
- Brown A.E.P., Costa E. C., 1972. Processing of a uraniferous zirconium ore. IEA Publication N. 274.
- Bruzzi L., Baroni M., Mazzotti G., Mele R., Righi S., 2000. Radioactivity in raw materials and end products in the Italian ceramics industry. *Journal of Environmental Radioactivity* 47, 171–181.
- Carvalho F.P., 1995.  $^{210}\text{Pb}$  and  $^{210}\text{Po}$  in sediments and suspended matter in the Tagus estuary, Portugal. Local enhancement of natural levels by wastes from phosphate ore processing industry. *The Science of the Total Environment* 159, 201–214.
- Cesana A., Terrani M., 1989. An empirical method for peak-to-total ratio computation of a gamma-ray detector. *Nuclear Instruments and Methods in Physics Research A* 281, 172–175.
- Condie K. C., 1993. Chemical composition and evolution of the upper continental crust: Contrasting results from surface samples and shales. *Chemical Geology* 104, 1–37.
- Cooper M.B., Clarke P.C., Robertson W., Mcpharlin I. R., Jeffrey R.C., 1995. An investigation of radionuclide uptake into food crops grown in soils treated with Bauxite mining residues. *Journal of Radioanalytical and Nuclear Chemistry* 194, 379–387.
- Currie L. A., 1986. Limits for Qualitative Detection and Quantitative Determination Application to Radiochemistry. *Analytical Chemistry* 40, 586–593.
- Cutshall N. H., Larsen I. L., Olsen C. R., 1983. Direct analysis of Pb-210 in sediment samples: self-absorption corrections. *Nuclear Instruments and Methods* 206, 309–312.
- DeFelice P., Fazio A., Vidmar T., Korun M., 2006. Close-geometry efficiency calibration of p-type HPGe detectors with a Cs-134 point source. *Applied Radiation and Isotopes* 64, 1303–1306.
- De Felice P., Angelini P., Fazio A., Biagini R., 2000. Fast procedures for coincidence-summing correction in gamma-ray spectrometry. *Applied Radiation and Isotopes* 52, 745–752.
- Döring J., Beck T., Beyermann M., Gerler J., Henze G., Mielcarek J., Schkade U.K., 2007. Exposure and radiation protection for work areas with enhanced natural radioactivity NORM V (Proc. Conf. Seville, Spain 2007).
- Dryák P. and Kovář P., 2009. Table for true summation effect in gamma-ray spectrometry. *Journal of Radioanalytical and Nuclear Chemistry* 279, 385–394.
- ECOBA European Coal Combustion Products Association, 2003. CCP Production & Use Survey - EU 15.
- El Afifi E.M., Hilal M.A., Attallah M.F., EL-Reefy S.A., 2009. Characterization of phosphogypsum wastes associated with phosphoric acid and fertilizers production. *Journal of Environmental Radioactivity* 100, 407–412.
- Flues M., Camargo I.M.C., Silva P.S.C., Mazzilli B.P., 2006. Radioactivity of coal and ashes from Figueira coal power plant in Brazil. *Journal of Radioanalytical and Nuclear Chemistry* 270, 597–602

- Gazineu M.H.P., Araújo A.A., Brandão Y.B., Hazin C.A., Godoy J.M., 2005. Radioactivity concentration in liquid and solid phases of scale and sludge generated in the petroleum industry. *Journal of Environmental Radioactivity* 81, 47–54.
- Gazineu M.H.P., Hazin C.A., 2008. Radium and potassium-40 in solid wastes from the oil industry. *Applied Radiation and Isotopes* 66, 90–94.
- Georgescu D., Aurelian F., Popescu M., Radulescu C., 2004. Sources of TENORM – Inventory of phosphate fertilizer and aluminium industry, NORM IV (Proc. Conf. Szczyrk, 2004).
- Godoy J.M., Cruz R.P., 2003.  $^{226}\text{Ra}$  and  $^{228}\text{Ra}$  in scale and sludge samples and their correlation with the chemical composition. *Journal of Environmental Radioactivity* 70, 199–206.
- Guimond R.J., Hardin J.M., 1989. Radioactivity Released from Phosphate-Containing Fertilizers and from Gypsum. *Radiation Physics Chemistry* 34, 309–315.
- Heaton B., Lambley J., 1995. TENORM in the Oil, Gas and Mineral Mining Industry. *Applied Radiation and Isotopes* 46, 577–581.
- Hind A.R., Bhargava S.K., Grocott S.C., 1999. The surface chemistry of Bayer process solids: a review. *Colloids and Surfaces A: Physicochemical and Engineering Aspects* 146, 359–374.
- Hull C.D., Burnett W.C., 1996. Radiochemistry of Florida Phosphogypsum. *Journal of Environmental Radioactivity* 32, 213–238.
- IAEA International Atomic Energy Agency, 2008. Naturally Occurring Radioactive Material (NORM V), Proceedings Series, IAEA, Vienna.
- IAEA International Atomic Energy Agency, 2003a. Radioactive Waste Management Glossary, IAEA, Vienna.
- IAEA International Atomic Energy Agency, 2003b. Extent of Environmental Contamination by Naturally Occurring Radioactive Material (NORM) and Technological Options for Mitigation, Technical Reports Series No. 419, IAEA, Vienna.
- IAEA International Atomic Energy Agency, 2006. Assessing the Need for Radiation Protection Measures in Work Involving Minerals and Raw Materials, Safety Reports Series No. 49, IAEA, Vienna.
- IAEA International Atomic Energy Agency, 1996. International Basic Safety Standards for Protection against Ionizing Radiation and for the Safety Radiation Sources, Safety Series No. 115, IAEA, Vienna.
- Jerez Vegueria S.F., Godoy J.M., Miekeley N., 2002. Environmental impact studies of barium and radium discharges by produced waters from the “Bacia de Campos” oil-field offshore platforms, Brazil. *Journal of Environmental Radioactivity* 62, 29–38.
- Jobbágy V., Somlai J., Kovács J., Szeiler G., Kovács T., 2009. Dependence of radon emanation of red mud bauxite processing wastes on heat treatment. *Journal of Hazardous Materials* 172, 1258–1263.
- Jonkers G., Hartog F.A., Knaepen A.A.I., Lancee P.F.J., 1997. Characterization of NORM in the oil and gas production (E&P) industry, Radiological Problems with Natural Radioactivity in the Non-Nuclear Industry (Proc. Int. Symp. Amsterdam).
- Knoll G.F., 1999. Radiation Detection and Measurements, Third Edition, John Wiley & Sons, 1999.
- Landais P., 1996. Organic geochemistry of sedimentary uranium ore deposits. *Ore Geology Reviews* 11, 33–51.
- Lysebo I., Birovljev A., Strand T., 1996. NORM in oil production – occupational doses and environmental aspects. Proceedings of the 11th Congress of the Nordic Radiation Protection Society, Reykjavik, Iceland.
- Mazzilli B., Palmiro V., Saueia C., Nisti M.B., 2000. Radiochemical characterization of Brazilian phosphogypsum. *Journal of Environmental Radioactivity* 49, 113–122.
- McNulty G.S., 2007. Production of titanium dioxide. (Proc. Conf. Seville, Spain 2007).
- Menzel R.G., 1968. Uranium, Radium, and Thorium Content in Phosphate Rocks and Their Possible Radiation Hazard. *Journal of Agricultural and Food Chemistry* 16, 231–234.
- Metz V., Kienzler B., Schüßler W., 2003. Geochemical evaluation of different groundwater–host rock systems for radioactive waste disposal. *Journal of Contaminant Hydrology* 61, 265–279.
- Moens L., De Donder J., Xi-lei L., De Corte F., De Wespelaere A., Simonits A., Hoste J., 1981. Calculation of the absolute peak efficiency of gamma-ray detectors for different counting geometries. *Nuclear Instruments and Methods* 187, 451–472.
- Monographie BIPM-5, 2004. Table of Radionuclides Vol-2. Bureau International des Poids et Mesure, ISBN 92-822-2207-1.
- Mukherjee A.B., Zevenhoven R., Bhattacharya P., Sajwan K.S., Kikuchi R., 2008. Mercury flow via coal and coal utilization by-products: A global perspective. *Resources, Conservation and Recycling* 52, 571–591.
- Nakashima S., 1992. Complexation and reduction of uranium by lignite. *The Science of the Total Environment* 117/118, 425–437.
- Omar M., Ali H.M., Abu M.P., Kontol K.M., Ahmad Z., Ahmad S.H.S.S., Sulaiman I., Hamzah R., 2004. Distribution of radium in oil and gas industry wastes from Malaysia. *Applied Radiation and Isotopes* 60, 779–782.
- Papatheodorou G., Papaefthymiou H., Maratou A., Ferentinos G., 2005. Natural radionuclides in bauxitic tailings (red-mud) in the Gulf of Corinth, Greece. *Radioprotection, Supplement 1*. 40, 549–555.

- Paschoa A.S., 2008. NORM from the Monazite Cycle and from the Oil and Gas Industry: Problems and tentative solutions. International Conference on Radioecology and Environmental Radioactivity. (Proc. Conf. Bergen, Norway 2008).
- Paschoa A.S., 1997. Potential Environmental and Regulatory Implications of Naturally Occurring Radioactive Materials (NORM). *Applied Radiation and Isotopes* 49, 189–196.
- Paschoa A.S., 1993. Overview of environmental and waste management aspects of the monazite cycle. *Radiation Protection in Australia* 11, 170–173.
- Philipsborn H.V., Kuhnast E., 1992. Gamma spectrometric characterization of industrially used African and Australian Bauxites and their red mud tailings. *Radiation Protection Dosimetry* 45, 741–744.
- Pinnock W., 1991. Measurements of radioactivity in Jamaican building materials and gamma dose equivalents in a prototype red mud house. *Health Physics* 61, 647–651.
- Pontikes Y., Vangelatos I., Boufounos D., Fafoutis D., Angelopoulos G.N., 2006. Environmental aspects on the use of Bayer's process Bauxite Residue in the production of ceramics. *Advances in Science and Technology* 45, 2176–2181.
- Poole A.J., Allington D.J., Baxter A.J., Young A.K., 1995. The natural radioactivity of phosphate ore and associated waste products discharged into the eastern Irish Sea from a phosphoric acid production plant. *The Science of the Total Environment* 173/174, 137–149.
- Righi S., Andretta M., Bruzzi L., 2005. Assessment of the radiological impacts of a zircon sand processing plant. *Journal of Environmental Radioactivity* 82, 237–250.
- Rubio Montero M.P., Durán Valle C.J., Jurado Vargas M., Botet Jiménez A., 2009. Radioactive content of charcoal. *Applied Radiation and Isotopes* 67, 953–956.
- Ruyters S., Mertens J., Vassilieva E., Dehandschutter B., Poffijn A., Smolders E., 2011. The Red Mud Accident in Ajka (Hungary): Plant Toxicity and Trace Metal Bioavailability in Red Mud Contaminated Soil. *Environmental Science and Technology* 45, 1616–1622.
- Santos A.J.G., Mazzilli B.P., Fávaro D.I.T., Silva P.S.C., 2006. Partitioning of radionuclides and trace elements in phosphogypsum and its source materials based on sequential extraction methods. *Journal of Environmental Radioactivity* 87, 52–61.
- Sauaia C.H., Mazzilli B.P., Fávaro D.I.T., 2005. Natural radioactivity in phosphate rock, phosphogypsum and phosphate fertilizers in Brazil. *Journal of Radioanalytical and Nuclear Chemistry* 264, 445–448.
- Sauaia C.H.R., Mazzilli B.P., 2006. Distribution of natural radionuclides in the production and use of phosphate fertilizers in Brazil. *Journal of Environmental Radioactivity* 89, 229–239.
- Shawky S., Amer H., Nada A.A., El-Maksoud T.M.A., Ibrahiem N.M., 2001. Characteristics of NORM in the oil industry from Eastern and Western deserts of Egypt. *Applied Radiation and Isotopes* 55, 135–139.
- Silva N.C., Fernandes E.A.N., Cipriani M., Taddei M.H.T., 2001. The natural radioactivity of Brazilian phosphogypsum. *Journal of Radioanalytical and Nuclear Chemistry* 249, 251–255.
- Smith M.L., Bignell L., Alexiev D., Mo L., HARRISO J., 2008 Evaluation of lead shielding for a gamma-spectroscopy system. *Nuclear Instruments and Methods in Physics Research A* 589, 275–279.
- Somlai J., Jobbágy V., Kovács J., Tarján S., Kovács T., 2008. Radiological aspects of the usability of red mud as building material additive. *Journal of Hazardous Materials* 150, 541–545
- Tadmor. J., 1986. Radioactivity From Coal-Fired Power Plants: a review. *Journal of Environmental Radioactivity* 4, 177–204.
- Tayibi H., Choura M., López F.A., Alguacil F.J., López-Delgado A., 2009. Environmental impact and management of phosphogypsum. *Journal of Environmental Management* 90, 2377–2386.
- Timmermans C.W.M., van der Steen J., 1996. Environmental and Occupational Impacts of Natural Radioactivity from Some Non-Nuclear Industries in The Netherlands. *Journal of Environmental Radioactivity* 32, 97–104.
- Tomarchio E. and Rizzo S., 2011. Coincidence-summing correction equations in gamma-ray spectrometry with p-type HPGe detectors. *Radiation Physics and Chemistry* 80, 318–323.
- Turhan S., Arikan I.H., Demirel H., Güngör N., 2011. Radiometric analysis of raw materials and end products in the Turkish ceramics industry. *Radiation Physics and Chemistry* 80, 620–625.
- UNSCEAR United Nations Scientific Committee on the Effects of Atomic radiation, 2000. Sources and effects of ionizing radiation. Report to the General Assembly of the United Nations with Scientific Annexes, United Nations sales publication E.00.IX.3, New York.
- U.S. EIA / IOE U.S. Energy Information Administration / International Energy Outlook 2010.
- USGS U.S. Geological Survey Data Series 140. Kelly, T., Buckingham, D., DiFrancesco, C., Porter, K., Goonan, T., Sznopce, J., Berry, C., and Crane, M., 2002, "Historical statistics for mineral commodities in the United States," U.S. Geological Survey open-file report 01-006, minerals.usgs.gov/minerals/pubs/of-01-006/.
- USGS MCS U.S. Geological Survey Mineral Commodities Summary, 1996.
- USGS MCS U.S. Geological Survey Mineral Commodities Summary, 2011.
- Zielinski R.A., Otton J.K., Budahn J.R., 2001. Use of radium isotopes to determine the age and origin of radioactive barite at oil-field production sites. *Environmental Pollution* 113, 299–309.

WCI World Coal Institute, Coal Facts 2005 Edition.